CSIAM Trans. Life Sci.
doi: 10.4208/csiam-ls.SO-2025-0020

Vol. **2**, No. 1, pp. 1-22
March 2026

The Dynamics of CD4+ T Cell Proliferation in Autopilot Model

Xiu Li[1,2], Meili Li[1] and Junling Ma[2,*]

[1] *School of Mathematics and Statistics, Donghua University, Shanghai 201620, China.*
[2] *Department of Mathematics and Statistics, University of Victoria, Victoria, BC, Canada.*

Received 15 June 2025; Accepted 17 August 2025

Abstract. Under the assumption of the autopilot model, after antigen stimulation exceeds a threshold, the proliferation and effector function of CD4+ T cells are self-sustained and do not need further antigen stimulation. However, CD4+ T cell proliferation is driven by their production of IL-2, which then binds to cells and triggers proliferation. Without regulation, this autocrine process forms a positive feedback loop that causes uncontrolled proliferation. This study mathematically modeled the regulatory mechanisms of the CD4+ T cell response after infection, focusing on the role of IL-2 self-regulation and Treg in this mechanism. We performed a phase-space analysis to study the long-term behavior of the proliferation process. Our results show that IL-2 self-regulation alone is not sufficient to fully inhibit CD4+ T cell response, and that the involvement of Treg cells is essential to regulate the immune response effectively. In particular, when the rate of CD4+ T cell proliferation is controlled by the rate of IL-2-mediated CD4+ T cell removal, Treg cells control CD4+ T cell proliferation by releasing immunosuppressive cytokines such as IL-10 and TGF-β, thus inhibiting the unregulated immune response.

AMS subject classifications: 92D25

Key words: Adaptive immune system, immune response, within-host, clonal expansion.

1 Introduction

CD4+ T cells are the principal coordinators of the adaptive immune system, governing both CD8+ T response and the antibody response. In a primary response, naive

*Corresponding author. *Email address:* junlingm@uvic.ca (J. Ma)

CD4+ T cells are activated when major histocompatibility complex class II molecules (MHC-II) on the surface of antigen presenting cells (APCs, such as dendritic cells) bind to T cell receptors (TCR) on CD4+ T cells. Full activation requires co-stimulatory molecules (such as CD28 and B7 family ligands) to produce a secondary signal that reduces invalid or self-responsiveness [23]. Upon activation, CD4+ T cells differentiate into different effector subpopulations (Th1, Th2, Th17, Treg) to influence the characteristics of the immune response [28]. This differentiation is driven by cytokines such as interleukin-6 (IL-6), interleukin-12 (IL-12), and transforming growth factor-beta (TGF-β).

Since the adaptive immune system can recognize an immense number of distinct antigens (in the order of 10^7 to 10^{14}) [19], only a tiny fraction of CD4+ T cells are activated. Thus, they must undergo a proliferation process to reach a sufficient level for effective function. This proliferation process significantly influences the magnitude and efficacy of the immune response, therefore determining the success or failure of viral clearance [10].

Interleukin-2 (IL-2) is a key driver for CD4+ T cell proliferation [2], and is primarily produced by CD4+ T cells [20]. This autocrine action of IL-2 in CD4+ T cells forms a positive feedback loop, which ensures the efficacy and duration of immune response through their rapid proliferation and functional maintenance [14, 18].

The duration of TCR stimulation must exceed a specific threshold for T cells to fully activate, start helper activities, and encourage cell proliferation. This threshold mechanism ensures effective recognition and robust response of the immune system to antigens, while preventing nonspecific activation by transient or weak stimuli [9, 12]. However, once the activation threshold is reached, T cells adopt a 'automatic driving' state, i.e. they maintain proliferation and effector activities without continued TCR stimulation after initial activation [13,24]. This phenomenon is referred to as the 'autopilot model' [1,3].

If appropriate negative controls are lacking, the autocrine action of IL-2 and CD4+ T cells in the autopilot model will result in uncontrolled proliferation, tissue damage and autoimmune diseases including multiple sclerosis [4, 15]. Thus, T cell proliferation must be regulated to prevent excessive immune activation and to mitigate immune-mediated tissue damage and inflammation. The adaptive immune system has multiple mechanisms for such regulation.

The main mechanism is provided by regulatory T (Treg) cells. Treg cells regulate the proliferation of activated CD4+ T cells via two cytokines: interleukin-10 (IL-10) and TGF-β. TGF-β promotes Treg differentiation while reducing the differentiation of helper phenotypes [5]. In addition, IL-10 inhibits antigen presentation of antigen-presenting cells. TGF-β and IL-10 also directly inhibit IL-2 production, whereby limiting CD4+ T cell proliferation. TGF-β does this via the Smad2/3 pathway which suppresses the activity of the transcription factor associated with the IL-2 gene promoter [25], while IL-10 directly suppresses critical transcription factors for IL-2 production (NF-κB and NFAT) via the STAT3 pathway [11]. Furthermore, TGF-β upregulates cell cycle inhibitors such as p21 and p27, inducing apoptosis in CD4+ T cells [27].

In addition, multiple self-regulating mechanisms of IL-2 guarantee that a high concentration of IL-2 has a negative impact on CD4+ T cell proliferation. For example, IL-2

activates the STAT5 pathway in these cells, which induces the transcription of Blimp-1 [22], thereby further reducing IL-2 production [8]. In addition, an increased IL-2 concentration may upregulate Fas/FasL expression and induce apoptosis [21].

Currently, the impact of these regulatory systems on the immunological feedback cycle remains ambiguous, which hinders the comprehension of the stability of the immune system. Mathematical models serve as a potent instrument, capable of incorporating various regulatory factors to simulate the dynamic processes of immune feedback. They quantify the effects of distinct mechanisms on the intensity and duration of immune responses, thereby offering valuable support for the investigation of immune regulation and disease treatment. Garcia-Martínez and León [7] presented a model that characterizes IL-2's regulatory role between helper T cells and Tregs. The model clarifies the multi-homeostatic states of tolerance and activation within the immune system, differentiates the various states of two T cell types, employs ordinary differential equations to characterize cell activation, proliferation, and IL-2 dynamics. Khailaie *et al.* [16] established a three-variable ordinary differential equation model combining IL-2, natural Tregs, and CD4+ T cells. Incorporating an intracellular suicide mechanism to limit the over-amplification of CD4+ T cells, the study applied the Hill function to characterize IL-2-dependent cell proliferation and saturation and showed complex dynamic events such as multi-stable states and bifurcation via numerical simulation. Pariya *et al.* [17] then developed a mathematical model integrating tumor cells, effector T cells, and Tregs; investigated the dynamic mechanism of Treg-mediated inhibition of effector T cells and its consequences in chemotherapy-immunotherapy; and proposed modulating Treg function as a feasible target for cancer immunotherapy. Cuesta-Herrera *et al.* [6] created a multivariate ODE model underlining how different immune cells and viruses interact during a viral infection, so stressing how regulatory T cells help govern CD4+ helper T cells and cytotoxic T cells. Emphasizing their vital contribution to reduce excessive inflammation and preserve immune homeostasis, the model shows how regulatory T cells inhibit immunological activation. Subsequently, Zhang *et al.* [26] improved the Khailaie model by using the Michaelis-Menten framework to refine the saturated proliferation of CD4+ T cells, eliminating the intracellular suicide mechanism, and stressing the analysis of the roles of natural Tregs (nTregs) and induced Tregs (iTregs). This work thoroughly described the dynamic mechanisms of threshold activation and immune clearance, using time-scale separation methods to simplify IL-2 dynamics.

The existing mathematical model did not consider the self-regulatory mechanism of IL-2. In addition, these models use simple mathematical terms (such as a mass-action killing term) to describe regulation, and did not consider the biological mechanisms of Treg regulation, such as inhibitory factors IL-10 and TGF-β. These limit the applicability of existing models to understand the complex interactions of regulatory mechanisms. Consequently, it is essential to develop more sophisticated mathematical models to study IL-2 self-regulation and Treg-mediated inhibition. In this paper, we develop novel mathematical models to incorporate these mechanisms and clarify their roles in immune feedback regulation through rigorous mathematical analysis, therefore providing

theoretical insights to support quantitative research and clinical intervention in immune regulation mechanisms.

2 Mathematical description of the autopilot model

To understand the dynamics of the autopilot model, we establish a mathematical model following the ideas of [26]. Assume that naive CD4+ T cells are activated at a rate of $\lambda_h(t)$ at time t. This rate depends on the viral load and mature dendritic cell dynamics, and thus is time dependent. The autopilot model depends on the following assumption [13, 24].

Autopilot model assumption. If the T cells are fully activated via an extended TCR exposure, their proliferation and effector activities do not need further TCR stimulation.

Denote the activated CD4+ T cells as T_h. Assume that T_h cells have a proliferation rate π_h and a natural death rate μ_h. The proliferation rate is assumed to saturate at a high concentration of IL-2 (denoted as I_2). This is modeled in the Michaelis-Menten form $(\pi_h T_h I_2/K_2)/(1+I_2/K_2)$ where K_2 is the IL-2 concentration that reduces the maximum (saturated) proliferation rate by half. We choose K_2 to be the unit of IL-2 concentration, i.e. set $K_2=1$. Assume that each T_h cell produces IL-2 at a rate ρ_2, and IL-2 is cleared at a rate c_2. Thus, the autopilot model can be written as

$$\frac{dT_h}{dt}=\lambda_h(t)+\frac{\pi_h I_2 T_h}{1+I_2}-\mu_h T_h, \tag{2.1a}$$

$$\frac{dI_2}{dt}=\rho_2 T_h-c_2 I_2. \tag{2.1b}$$

After the removal of TCR stimulation, naive CD4+ T cells are no longer activated. At this time (denoted at $t=0$), the system has a positive initial condition $T_h(0)>0$ and $I_2(0)>0$, and $\lambda_h(t)=0$ for all $t\geq 0$. Thus, model (2.1) is simplified to

$$\frac{dT_h}{dt}=\frac{\pi_h I_2 T_h}{1+I_2}-\mu_h T_h, \tag{2.2a}$$

$$\frac{dI_2}{dt}=\rho_2 T_h-c_2 I_2. \tag{2.2b}$$

Note that this is a special case of the Zhang *et al.* [26] model, in which Treg cells are ignored. In [26], it has been shown that $\pi_h>\mu_h$ allows a fast CD4+ T cell response. It was also found that the solution may become unbounded. This can be quickly verified by conducting a time-scale separation similar to that in [26]. The IL-2 dynamics are much faster than the T_h dynamics, i.e. ρ_2 and c_2 are much faster than π_h and μ_h; thus, we can assume that IL-2 approaches the quasi-equilibrium

$$I_2^*=\frac{\rho_2 T_h}{c_2}.$$

Substituting this into the Eq. (2.2a) gives

$$\frac{dT_h}{dt} = \frac{\pi_h \rho_2 T_h^2}{c_2 + \rho_2 T_h} - \mu_h T_h. \tag{2.3}$$

This equation has two equilibria if $\pi_h > \mu_h$. The origin $E_0 = 0$ is locally asymptotically stable, and the positive equilibrium

$$E^+ = \frac{c_2 \mu_h}{(\pi_h - \mu_h)\rho_2}$$

is unstable. Thus, if the initial condition $T_h(0) > E^+$, then the solution approaches ∞. This is the key feature of a positive feedback loop, which allows fast growth. However, if the loop is not regulated, the solutions become unbounded.

Note that the time-scale separation is not needed. A simple phase-plane analysis of the original system yields the same outcome. There are two equilibria in the first quadrant, the origin is locally asymptotically stable, and the positive equilibrium is a saddle. If the initial condition is above the stable manifold of the saddle point, the solution approaches infinity. The details are omitted here as the calculations are straightforward. However, we will use time-scale separation throughout because it greatly simplifies the calculations while being biologically realistic.

In the following sections, we incorporate biological mechanisms that limit the growth of T_h and break the positive loop.

3 IL-2 self-regulation

In this section, we study the effect of the negative feedback of IL-2 on the proliferation of CD4+ T cells. As we mentioned in the Introduction, multiple mechanisms separately guarantee that a high IL-2 concentration does not lead to uncontrolled CD4+ proliferation. In this section, we focus on two main mechanisms.

3.1 Inhibiting IL-2 production in CD4+ T cells

To model this, we assume that the IL-2 production rate decreases as a function of I_2, i.e. $\rho_2/(1+\kappa_2 I_2)$, where $1/\kappa_2$ is the IL-2 concentration that reduces the maximum production rate by half. The model can be written as

$$\frac{dT_h}{dt} = \frac{\pi_h I_2 T_h}{1 + I_2} - \mu_h T_h, \tag{3.1a}$$

$$\frac{dI_2}{dt} = \frac{\rho_2}{1+\kappa_2 I_2} T_h - c_2 I_2. \tag{3.1b}$$

In this subsection, again we assume that the proliferation rate of activated CD4+ T cells is greater than their natural death rates. i.e. $\pi_h > \mu_h$. We also conduct a time-

scale separation, and assume that the IL-2 dynamics is a fast process and approaches a quasi-equilibrium I_2^* that satisfies

$$\frac{\rho_2}{1+\kappa_2 I_2} T_h - c_2 I_2 = 0.$$

This can be simplified to a quadratic equation of the form

$$\rho_2 T_h - c_2 I_2 - c_2 \kappa_2 I_2^2 = 0,$$

which has a unique positive root

$$I_2^*(T_h) = \frac{-c_2 + \sqrt{c_2^2 + 4c_2\kappa_2\rho_2 T_h}}{2c_2\kappa_2}.$$

Substituting this into (3.1a), the slow T cell dynamics becomes

$$\frac{dT_h}{dt} = \frac{\pi_h I_2^*(T_h) T_h}{1+I_2^*(T_h)} - \mu_h T_h. \tag{3.2}$$

This equation also has two equilibria. The origin $E_0 = 0$ is locally asymptotically stable, and the positive equilibrium T_h^* satisfies

$$\frac{I_2^*(T_h^*)}{1+I_2^*(T_h^*)} = \frac{\mu_h}{\pi_h},$$

and thus

$$I_2^*(T_h^*) = \frac{-c_2 + \sqrt{c_2^2 + 4c_2\kappa_2\rho_2 T_h^*}}{2c_2\kappa_2} = \frac{\mu_h}{\pi_h - \mu_h}. \tag{3.3}$$

This gives

$$T_h^* = \frac{\mu_h c_2 [\pi_h + (\kappa_2 - 1)\mu_h]}{\rho_2 (\pi_h - \mu_h)^2},$$

which is unstable.

Thus, if the initial condition $T_h(0) > T_h^*$, the solution approaches ∞. This shows that self-inhibition of IL-2 production cannot limit the growth of T_h population.

3.2 Increasing CD4+ T cell apoptosis

We incorporate this mechanism in the above model, assuming that T_h cells have a maximum excess death rate d_2 when the IL-2 concentration saturates. Thus,

$$\frac{dT_h}{dt} = \frac{\pi_h I_2 T_h}{1+I_2} - \mu_h T_h - d_2 \frac{\eta_2 I_2}{1+\eta_2 I_2} T_h, \tag{3.4a}$$

$$\frac{dI_2}{dt} = \frac{\rho_2}{1+\kappa_2 I_2} T_h - c_2 I_2, \tag{3.4b}$$

where $1/\eta_2$ is the IL-2 concentration that causes the excess death rate to reach $d_2/2$.

As in previous sections, we again perform a time scale separation: Assuming that I_2 reaches a quasi-equilibrium I_2^* given by (3.3). Then model (3.4) is simplified to

$$\frac{dT_h}{dt}=\frac{\pi_h I_2^* T_h}{1+I_2^*}-\mu_h T_h-d_2\frac{\eta_2 I_2^*}{1+\eta_2 I_2^*}T_h. \tag{3.5}$$

The origin $E_0=0$ is also locally asymptotically stable. Positive equilibrium satisfy

$$\frac{\pi_h I_2^*}{1+I_2^*}-\mu_h-d_2\frac{\eta_2 I_2^*}{1+\eta_2 I_2^*}=0.$$

This simplifies to a quadratic equation on I_2^*,

$$(\pi_h-\mu_h-d_2)\eta_2 I_2^{*2}+(\pi_h-\mu_h-\mu_h\eta_2-d_2\eta_2)I_2^*-\mu_h=:AI_2^{*2}+BI_2^*-\mu_h=0.$$

Case 1: If $\pi_h>\mu_h+d_2$, then there exists a single positive equilibrium

$$I_2^*=\frac{-B+\sqrt{B^2+4\mu_h A}}{2A}.$$

This corresponds to a unique positive equilibrium, T_h^*, which is unstable. This case is thus similar to the discussion in Section 3.1, where the solution approaches ∞ if $T_h(0)>T_h^*$. Thus, if the proliferation rate π_h exceeds the maximum total death rate μ_h+d_2, the proliferation cannot be regulated.

Case 2: If $A<0<B$ and $B^2+4\mu_h A>0$, i.e.

$$\begin{aligned}&\mu_h+\mu_h\eta_2+d_2\eta_2<\pi_h<\mu_h+d_2,\\&(\pi_h-\mu_h-\mu_h\eta_2-d_2\eta_2)^2+4\mu_h\eta_2(\pi_h-\mu_h-d_2)>0,\end{aligned}$$

then there exist two positive equilibria,

$$E^{\pm}=\frac{-B\pm\sqrt{B^2+4\mu_h A}}{2A},$$

where the smaller equilibrium E^- is unstable, and the larger equilibrium E^+ is locally asymptotically stable. Thus, if the initial condition $T_h(0)>E^-$, the solution approaches E^+ as $t\to\infty$. On the other hand, if $T_h(0)<E^-$, then the solution approaches the origin monotonically.

Case 3: If $A<0<B$ and $B^2+4\mu_h A<0$, i.e.

$$\begin{aligned}&\mu_h+\mu_h\eta_2+d_2\eta_2<\pi_h<\mu_h+d_2,\\&(\pi_h-\mu_h-\mu_h\eta_2-d_2\eta_2)^2+4\mu_h\eta_2(\pi_h-\mu_h-d_2)<0.\end{aligned}$$

In this case, there is no positive equilibrium, and all solutions with a positive initial condition decrease monotonically to the origin with respect to time t. In this case, the response is solely driven by the activation of naive CD4+ T cells. Without activation, the response immediately dies out, which is against the autopilot model assumption.

In summary, only Cases 1 and 2 are compatible with the autopilot model assumption. These two cases are distinguishable by the relative magnitude of the proliferation rate π_h and the maximum cell mortality μ_h+d_2. If the proliferation rate is larger, then there will be a large CD4+ T cell response. However, the increased T_h mortality driven by IL-2 cannot regulate the response, leading to uncontrollable proliferation. On the other hand, if the proliferation rate is lower, then the increased mortality stabilizes the IL-2 concentration if the activation exceeds the threshold E^-, but the response cannot be cleared after activation ceases. This suggests that Tregs are essential for clearing the CD4+ T cell response post viral clearance. We will study the regulation mechanism of Tregs in the following section.

4 Regulation of CD4+ T cell response by Tregs

As stated in Introduction, Tregs (denoted as T_R) regulate CD4+ T cell proliferation through multiple mechanisms. In this section, we consider two main regulatory mechanisms. First, Tregs produce TGF-β (denoted as I_β), which binds to CD4+ T cells and directly activates apoptosis pathways in CD4+ T cells. This results in an increase in the mortality of CD4+ T cells. We assume that this excess mortality occurs at a rate of $\gamma I_\beta/(1+I_\beta)$, where γ is the maximum excess mortality of activated CD4+ T cells. We choose the unit of TGF-β concentration such that the excess mortality is $\gamma/2$ at this concentration. In addition, Tregs also produce IL-10 (denoted as I_{10}). Both IL-10 and TGF-β (denoted as I_β) bind to activated CD4+ T cells and stop them from producing IL-2. Although these cells maintain their effector functions and do not die, they are removed from the T_h class, as this class is the producer of IL-2 in our model. We denote the removal rate per T_h cell as $\alpha_{10}\eta_{10}I_{10}/(1+\eta_{10}I_{10})$ and $\alpha_\beta\eta_\beta I_\beta/(1+\eta_\beta I_\beta)$, respectively, where α_{10} and α_β are the maximum removal rate; $1/\eta_\beta$ is the concentration of TGF-β at which the removal rate caused by TGF-β is reduced to $\alpha_\beta/2$. $1/\eta_{10}$ is IL-10 concentration such that the removal rate caused by IL-10 at this concentration is reduced to $\alpha_{10}/2$.

Tregs also limit the activation and differentiation of CD4+ T cells. However, under the assumption of the autopilot model, once activated, the proliferation of activated CD4+ T cells is independent of differentiation and activation signals. Therefore, this mechanism is not considered here.

Let π_R be the proliferation rate of Tregs, and μ_R be their natural death rate. We let ρ_β and ρ_{10} represent the production rate of TGF-β and IL-10 by Tregs, and c_β and c_{10} be their clearance rates, respectively. For simplicity, the two mechanisms of IL-2 self-regulation discussed in the previous section are omitted here. Similar to the activation term in the T_h equation discussed in previous sections, the activation term for Tregs is also ignored, and activation is considered as an initial perturbation from the origin. The model for Treg-mediated regulation of the CD4+ T cell response is written as

$$\frac{dT_h}{dt}=\frac{\pi_h I_2 T_h}{1+I_2}-\frac{\gamma I_\beta T_h}{1+I_\beta}-\frac{\alpha_{10}\eta_{10}I_{10}T_h}{1+\eta_{10}I_{10}}-\frac{\alpha_\beta\eta_\beta I_\beta T_h}{1+\eta_\beta I_\beta}-\mu_h T_h,$$

$$\begin{aligned}
&\frac{dI_2}{dt}=\rho_2 T_h-c_2 I_2,\\
&\frac{dT_R}{dt}=\frac{\pi_R I_2 T_R}{1+I_2}-\mu_R T_R,\\
&\frac{dI_{10}}{dt}=\rho_{10} T_R-c_{10} I_{10},\\
&\frac{dI_\beta}{dt}=\rho_\beta T_R-c_\beta I_\beta.
\end{aligned}$$

Similar to the preceding subsections, we again conduct a time scale separation: Providing that I_2, I_{10}, I_β attain the quasi-equilibrium states

$$I_2^*=\frac{\rho_2 T_h}{c_2},\quad I_\beta^*=\frac{\rho_\beta T_R}{c_\beta},\quad I_{10}^*=\frac{\rho_{10} T_R}{c_{10}},$$

and then substitute these into the rest equations gives

$$\frac{dT_h}{dt}=\frac{\pi_h\rho_2 T_h^2}{c_2+\rho_2 T_h}-\frac{\alpha_{10}\eta_{10}\rho_{10} T_h T_R}{c_{10}+\eta_{10}\rho_{10} T_R}-\frac{\alpha_\beta\eta_\beta\rho_\beta T_h T_R}{c_\beta+\eta_\beta\rho_\beta T_R}-\frac{\gamma\rho_\beta T_h T_R}{c_\beta+\rho_\beta T_R}-\mu_h T_h, \tag{4.1a}$$

$$\frac{dT_R}{dt}=\frac{\pi_R\rho_2 T_h T_R}{c_2+\rho_2 T_h}-\mu_R T_R. \tag{4.1b}$$

Theorem 4.1. *Model* (4.1) *does not exhibit closed orbits.*

Proof. We apply the Dulac's criterion. Let the right-hand sides of equations be denoted as F_{T_h} and F_{T_R}, corresponding to the rates of change of the variables T_h and T_R, respectively. Let

$$\Omega:=\left\{(T_h,T_R)\in\mathbb{R}^2 \mid T_h>0, T_R>0\right\}$$

the open first quadrant in the (T_h,T_R)-plane. Because negative coordinates are biologically inadmissible, every trajectory of model (4.1) remains in Ω. The set Ω is open, connected, and simply connected. Consider the function $\varphi=1/(T_h T_R)$. Next, we compute the divergence of the vector field $(\varphi F_{T_h},\varphi F_{T_R})$

$$\frac{\partial}{\partial T_h}(\varphi_1 F_{T_h})+\frac{\partial}{\partial T_R}(\varphi_1 F_{T_R})=\frac{\pi_h\rho_2 c_2}{T_R(c_2+\rho_2 T_h)^2}>0.$$

Since the divergence is strictly positive in the domain of interest, Dulac's criterion implies that the system cannot possess any closed orbit. □

The T_h nullclines are $T_h=0$ and

$$\frac{\pi_h\rho_2 T_h}{c_2+\rho_2 T_h}=\frac{\alpha_{10}\eta_{10}\rho_{10} T_R}{c_{10}+\eta_{10}\rho_{10} T_R}+\frac{\alpha_\beta\eta_\beta\rho_\beta T_R}{c_\beta+\eta_\beta\rho_\beta T_R}+\frac{\gamma\rho_\beta T_R}{c_\beta+\rho_\beta T_R}+\mu_h=:F(T_R). \tag{4.2}$$

Note that $F(T_R)$ is an increasing function. Thus,

$$T_h = \frac{c_2 F(T_R)/\pi_h}{\rho_2[1-F(T_R)/\pi_h]}. \tag{4.3}$$

The T_R nullclines are $T_R = 0$ and

$$\frac{\pi_R \rho_2 T_h}{c_2+\rho_2 T_h} = \mu_R,$$

that is, the nullcline is a horizontal line

$$T_h = \frac{c_2 \mu_R}{\rho_2(\pi_R-\mu_R)}. \tag{4.4}$$

Note that the origin $E_0=(0,0)$ is always an equilibrium. The Jacobian matrix of model (4.1) about E_0 is

$$\begin{bmatrix} -\mu_h & 0 \\ 0 & -\mu_R \end{bmatrix},$$

which corresponds to two negative eigenvalues. Thus, E_0 is always locally asymptotically stable. The existence of other equilibria in the first quadrant depends on the parameter values.

4.1 Case 1: $\pi_h < \mu_h$

In this case, the proliferation of activated CD4 + T cells is slower than their deaths. Note that $dT_h/dt < 0$ everywhere in the first quadrant and there are no boundary or positive equilibrium in the first quadrant except the origin E_0.

Subcase 1.1. $\pi_R < \mu_R$

In this subcase, the T_R nullcline (4.4) is not in the first quadrant either, and $dT_R/dt < 0$ everywhere in the first quadrant. Thus, the orbits in the first quadrant are positively bounded, and the Poincaré-Bendixson theorem guarantees that the origin E_0 is globally asymptotically stable in the first quadrant.

Subcase 1.2. $\pi_R > \mu_R$

In this subcase, the T_R nullcline (4.4) is in the first quadrant. In addition, $dT_R/dt > 0$ everywhere above the nullcline, and $dT_R/dt < 0$ everywhere below it. Thus, for orbits starting above this nullcline, T_R increases while T_h decreases, and so the orbit eventually crosses the nullcline to below it, where both T_h and T_R decrease. Like in Subcase 1.1, all orbits starting in the first quadrant are positively bounded, and thus the origin E_0 is globally asymptotically stable in the first quadrant. The phase portrait is illustrated in Fig. 1.

The following theorem summarizes this case. Biologically, this indicates that the immune system is incapable of initiating a fast and sufficient CD4+ T cell proliferation.

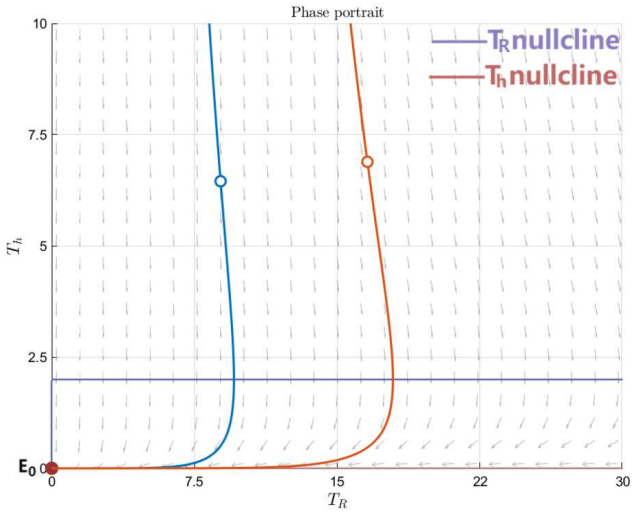

Figure 1: Phase portrait of model (4.1) under Subcase 1.2 of Case 1 (see Section 4.1), corresponding to the parameter regime where $\pi_h<\mu_h$ and $\pi_R>\mu_R$. The parameters are set as $\pi_R=0.2,\mu_R=0.1,\pi_h=0.4,\mu_h=0.6$. In this subcase, the T_h-nullcline coincides with the T_R-axis. The hollow circle designates the system's state at $t=0$, the same notation applies implicitly in all subsequent phase-plane plots. Under this configuration, all trajectories converge asymptotically to the origin.

Theorem 4.2. *If $\pi_h<\mu_h$, then the origin E_0 is globally asymptotically stable in the first quadrant, and T_h monotonically decreases to 0 with respect to time t for all solutions starting in this quadrant.*

4.2 Case 2: $\mu_h<\pi_h<\alpha_{10}+\alpha_\beta+\gamma+\mu_h$.

In this case, note that the increasing function $F(T_R)$ defined in (4.2) satisfies $F(0)=\mu_h<\pi_h$, and

$$F(\infty)=\alpha_{10}+\alpha_\beta+\gamma+\mu_h>\pi_h,$$

and thus there exists a unique $T_R^\infty>0$ such that $F(T_R^\infty)=\pi_h$, and the T_h nullcline defined in (4.3) has a vertical asymptote at $T_R=T_R^\infty$. This nullcline in the first quadrant for $0\le T_R\le T_R^\infty$.

In fact, as long as $\mu_h<\pi_h$, this T_h nullcline intersects with the T_R nullcline $T_R=0$ giving a boundary equilibrium in the first quadrant

$$E_b=(T_h^0,0),\quad T_h^0:=\frac{c_2\mu_h}{\rho_2(\pi_h-\mu_h)}. \tag{4.5}$$

The Jacobian of model (4.1) at this equilibrium is

$$\begin{bmatrix} \dfrac{\pi_h\rho_2T_h^0}{\left(c_2+\rho_2T_h^0\right)^2} & -\dfrac{\alpha_{10}\eta_{10}\rho_{10}T_h^0}{c_{10}}-\dfrac{\alpha_\beta\eta_\beta\rho_\beta T_h^0}{c_\beta}-\dfrac{\gamma\rho_\beta T_h^0}{c_\beta} \\ 0 & \dfrac{\pi_R\rho_2T_h^0}{c_2+\rho_2T_h^0}-\mu_R \end{bmatrix}. \tag{4.6}$$

Note that the two eigenvalues

$$\lambda_1 = \frac{\pi_h \rho_2 T_h^0}{\left(c_2 + \rho_2 T_h^0\right)^2} > 0,$$
$$\lambda_2 = \frac{\pi_R \rho_2 T_h^0}{c_2 + \rho_2 T_h^0} - \mu_R = \frac{1}{\pi_R}\left(\frac{\mu_h}{\pi_h} - \frac{\mu_R}{\pi_R}\right). \tag{4.7}$$

Thus, if $\mu_h/\pi_h < \mu_R/\pi_R$, then E_b is a saddle. On the other hand if, $\mu_h/\pi_h > \mu_R/\pi_R$, it is an unstable node.

To fully understand the behavior of model (4.1) in this case, we consider the following three subcases.

Subcase 2.1: $\pi_R < \mu_R$

Like Subcase 1.1, the T_R nullcline (4.4) is not in the first quadrant, and $dT_R/dt < 0$ for all orbits in the first quadrant.

Proposition 4.1. *In this subcase, the boundary equilibrium E_b is a saddle, and its stable manifold in the first quadrant $w_+^s(E_b)$ is below the T_h nullcline* (4.3)*, and has a positive slope in the quadrant.*

Proof. In this subcase, the boundary equilibrium E_b is a saddle because

$$\frac{\mu_h}{\pi_h} < 1 < \frac{\mu_R}{\pi_R},$$

and thus the eigenvalue of the Jacobian $\lambda_2 < 0$. The associated eigenvector has a positive slope. Thus, the first quadrant, which is an invariant set of model (4.1), must contain half of the stable manifold (denoted as $w_+^s(E_b)$).

If this $w_+^s(E_b)$ intersects with the T_h nullcline (4.3) at $T_h = A \geq 0$ in the first quadrant and lies above this nullcline for a small interval $T_h \in [A, A+\varepsilon]$, then, the region bounded by the nullcline, the stable manifold, and $T_h \leq A+\varepsilon$ form a Poincaré-Bendixson region, and this $A=0$ (i.e. the intersection is the equilibrium E_b), and all orbits in the region enters E_b, contradicting the fact that E_b is a saddle. This contradiction guarantees that $w_+^s(E_b)$ must be always below the T_h nullcline in the first quadrant. □

This proposition guarantees that the T_h nullcline and the stable manifold $w_+^s(E_b)$ divide the first quadrant into three regions: above the nullcline (denoted as Region I), between the nullcline and $w_+^s(E_b)$ (denoted as Region II), and below $w_+^s(E_b)$ (denoted as Region III). The orbits in Region I have $dT_h/dt > 0$ and $dT_R/dt < 0$ and thus approach ∞ along the T_h axis. The orbits in Region II have $dT_h/dt < 0$ and $dT_R/dt < 0$, but they are also bounded below by $w_+^s(E_b)$ which is invariant. Thus, these orbits must eventually enter Region I and approach ∞. The orbits in Region III have $dT_h/dt < 0$ and $dT_R/dt < 0$. Thus, the same arguments from Subcases 1.1 and 1.2 guarantee that these orbits approach the origin monotonically. The phase portrait is illustrated in Fig. 2.

That is, orbits starting above $w_+^s(E_b)$ approach ∞ while those starting below $w_+^s(E_b)$ approach the origin E_0 monotonically.

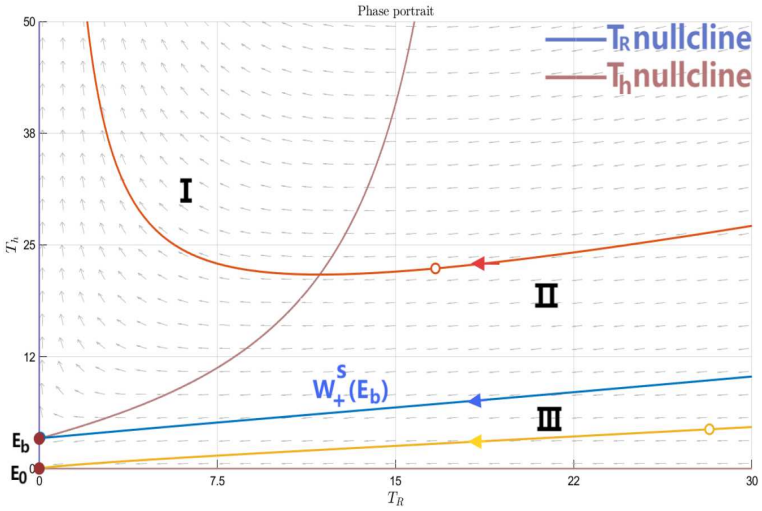

Figure 2: Phase portrait of model (4.1) under Subcases 2.1 of Case 2,corresponding to the parameter regime where $\mu_h<\pi_h<\alpha_{10}+\alpha_\beta+\gamma+\mu_h$ and $\pi_R<\mu_R$. For parameter values $\pi_R=0.2, \mu_R=0.3, \pi_h=0.4, \mu_h=0.25$, $\alpha_{10}=\alpha_\beta=\gamma=0.1$. Within region III, all orbits (except the stable manifold of E_b) converge to the origin asymptotically.

Subcase 2.2: $\mu_h/\pi_h<\mu_R/\pi_R<1$

In this subcase, the T_R nullcline (4.4) is in the first quadrant, the equilibrium E_b is still a saddle, which is below the T_R nullcline, and there exists a positive equilibrium $E^*=(T_h^*,T_R^*)$.

The two nullclines divide the phase space into four regions. Region I is bounded between the two nullclines and the T_h axis; Region II is above both nullclines (thus above Region I); Region III is above the T_R nullcline and to the right of the T_h nullcline (thus to the right of Region II); Region IV is below both nullclines (and thus below Regions I and III). These four regions are oriented counter-clockwise around the positive equilibrium E^*.

In Region I, $dT_h/dt>0$ and $dT_R/dt<0$. Thus, orbits starting in this region must move upward and left, eventually entering Region II, because they are bounded on the left by the invariant T_h axis. In Region II, $dT_h/dt>0$ and $dT_R/dt>0$. Thus, orbits starting in this region must cross the T_h nullcline (which has a vertical asymptote) and enter Region III. In Region III, $dT_h/dt<0$ and $dT_R/dt>0$. Thus, all orbits starting in this region must cross the T_R nullcline which is a horizontal line, and enter Region IV. In Region IV, $dT_h/dt<0$ and $dT_R/dt<0$. Thus, like Region III in Subcase 2.1, all orbits in Region IV must approach the origin monotonically (except for the stable manifold $w^s_+(E_b)$). Note that the positive equilibrium is unstable. The phase portrait is illustrated in Fig. 3.

Thus, in this subcase, all orbits except $w^s_+(E_b)$ in the first quadrant must eventually enter the origin E_0. For orbits above $w^s_+(E_b)$, T_h must first increase, then peak as the orbit intersects with the T_h nullcline, then decrease monotonically with respect to time t to 0. This corresponds to a fast CD4+ T cell response. In addition, for the orbits below $w^s_+(E_b)$,

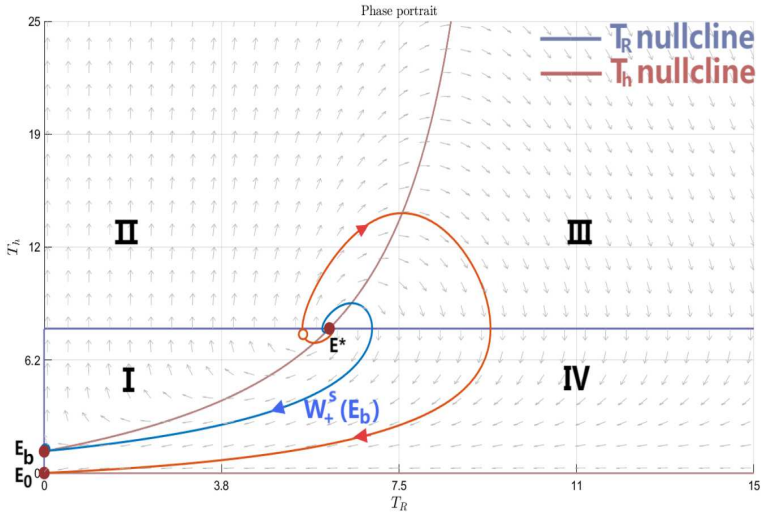

Figure 3: Phase portrait of model (4.1) under Subcase 2.2 of Case 2, where the parameters satisfy $\mu_h < \pi_h < \alpha_{10}+\alpha_\beta+\gamma+\mu_h$ and $\mu_h/\pi_h < \mu_R/\pi_R < 1$.The values used are $\pi_R = 0.2, \mu_R = 0.16, \pi_h = 0.4, \mu_h = 0.15, \alpha_{10} = \alpha_\beta = 0.4, \gamma = 0.1$. The stable manifold of E_b intersects the T_R-nullcline at E^*, while all other trajectories approach the origin.

$T_h(t)$ must decrease monotonically to 0, corresponding to no significant CD4+ T cell response. Thus, in this subcase, the CD4+ T cell response is an excitable response: The immune response is self-sustainable if and only if the activated CD4+ T cell population reaches a threshold (i.e. if it is above $w^s_+(E_b)$).

Subcase 2.3: $\mu_R/\pi_R < \mu_h/\pi_h < 1$

In this case, the T_h nullcline (4.3), which includes the boundary equilibrium E_b, is above the T_R nullcline (4.4). There is no positive equilibrium, and the boundary equilibrium E_b is an unstable node because $\lambda_2 > 0$. The T_h and T_R nullclines divide the first quadrant into three regions. Region I is above both nullclines, Region II is between the two nullclines, and Region III is below the two nullclines.

In Region I, $dT_h/dt > 0$ and $dT_R/dt > 0$, thus orbits in this region must move upward and to the right, eventually crossing the T_h nullcline to enter Region II, as the nullcline has a vertical asymptote. In Region II, $dT_h/dt < 0$ and $dT_R/dt > 0$, thus orbits in this region must move downward and to the right, crossing the T_h nullcline (which is horizontal) to enter Region III. In Region III, $dT_h/dt < 0$ and $dT_R/dt < 0$. Thus, as in Region III in Subcase 2.1, orbits in this region must enter the origin monotonically. The phase portrait is illustrated in Fig. 4.

Thus, the origin is globally asymptotically stable within the first quadrant. For orbits above the T_h nullcline (4.3), $T_h(t)$ must first increase, then peak when the orbit intersects with the $T_h(t)$ nullcline, and then decrease to 0 monotonically, corresponding to a CD4+

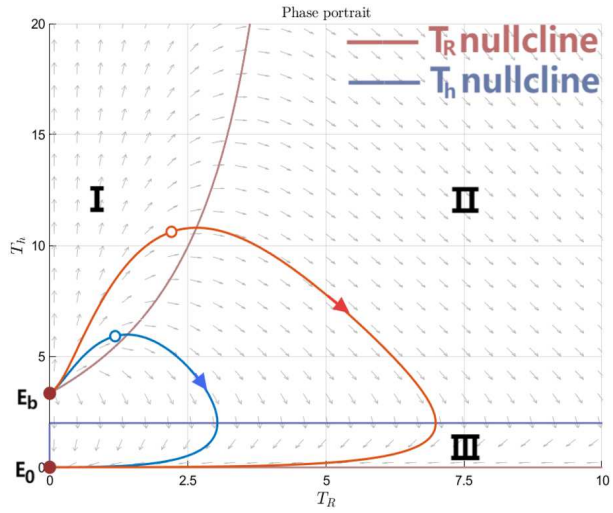

Figure 4: Phase portrait of model (4.1) under Subcase 2.3 of Case 2, where the parameters satisfy $\mu_h<\pi_h<\alpha_{10}+\alpha_\beta+\gamma+\mu_h$ and $\mu_R/\pi_R<\mu_h/\pi_h<1$. The values used are $\pi_R=0.2,\mu_R=0.1,\pi_h=0.4,\mu_h=0.25,\alpha_{10}=\alpha_\beta=0.4,\gamma=0.1$.

T cell response. For orbits below the T_h nullcline, $T_h(t)$ must monotonically decrease to 0 with respect to time t, which corresponds to no significant CD4+ response. Thus, like in Subcase 2.2, the CD4+ response is excitable.

The following Theorem summarizes the dynamics of model (4.1) in Case 2. Specifically, if Treg cells proliferate faster than their deaths, the CD4+ T cell response is excitable. Otherwise, there is no significant CD4+ T cell response occurs.

Theorem 4.3. *In Case* 2*, if* $\pi_h<\mu_h$*, then* $T_h(t)$ *monotonically decreases to* 0 *with respect to time* t *for all orbits in the first quadrant. If* $\pi_h>\mu_h$*, then there exists a curve in the first quadrant such that* $T_h(t)$ *monotonically decreases to* 0 *with respect to time* t *if the initial condition* $(T_h(0),T_R(0))$ *is below the curve. If the initial condition is above the curve,* $T_h(t)$ *first increases, then peaks, and finally decreases to* 0*.*

4.3 Case 3: $\pi_h>\alpha_{10}+\alpha_\beta+\gamma+\mu_h$

In this case, the T_h nullcline (4.3) is a positive monotonically increasing function of T_R. and saturated at

$$T_h^\infty=\frac{c_2(\alpha_{10}+\alpha_\beta+\gamma+\mu_h)/\pi_h}{\rho_2[1-(\alpha_{10}+\alpha_\beta+\gamma+\mu_h)/\pi_h]}.$$

Note that $T_h=T_h^\infty$ is a horizontal asymptote of this nullcline. In this case, the boundary equilibrium E_b still exists.

Like in Case 2, the dynamics of model (4.1) depends on the magnitude of μ_R/π_R. In this case, it can be categorized into the following four subcases.

4.3.1 Subcase 3.1: $\pi_R < \mu_R$

Like in Subcase 2.1, the T_R nullcline is not in the first quadrant, and the boundary equilibrium E_b exists and is a saddle; the stable manifold $w^s_+(E_b)$ must lie below the T_h nullcline. Thus, T_h nullcline and $w^s_+(E_b)$ divide the first quadrant into three regions. Region I is above both the nullcline and $w^s_+(E_b)$, Region II is between the nullcline and $w^s_+(E_b)$, Region III is below both. And like in Subcase 2.1, orbits above $w^s_+(E_b)$ approach ∞ along the T_h axis, while orbits below it approach the origin E_0 monotonically. The phase portrait is illustrated in Fig. 5.

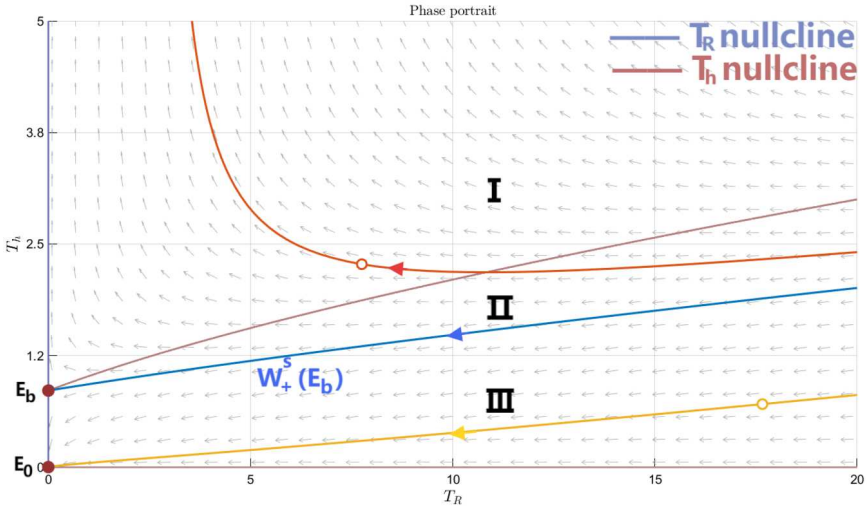

Figure 5: Phase portrait of model (4.1) under Subcase 3.1 of Case 3, where the parameters satisfy $\pi_h > \alpha_{10}+\alpha_\beta+\gamma+\mu_h$ and $\pi_R < \mu_R$. The values used are $\pi_R = 0.1, \mu_R = 0.2, \pi_h = 0.5, \mu_h = 0.15, \alpha_{10} = \alpha_\beta = \gamma = 0.1$.

4.3.2 Subcase 3.2: $\mu_R/\pi_R < \mu_h/\pi_h < 1$

Like in Subcase 2.3, the T_h nullcline (4.3) is above the T_R nullcline (4.4) in the first quadrant, and thus there is no positive equilibrium. The boundary equilibrium E_b is an unstable node. The horizontal asymptote $T_h = T_h^\infty$ of the T_h nullcline and the two nullclines divide the first quadrant into four regions. Region I is above the horizontal asymptote, Region II is between the asymptote and the T_h nullcline, Region III is between the two nullclines, Region IV is below both nullclines.

In Regions I and II, $dT_h/dt > 0$ and $dT_R/dt > 0$. Thus, in Region I, both $T_h(t)$ and $T_R(t)$ approach ∞ monotonically. In Region II, the orbits may either enter Region I or Region III. The boundary of these two behaviors is the trajectory Γ that leaves E_b such that $T_h = T_h^\infty$. In Region III, $dT_h/dt < 0$ and $dT_R/dt > 0$. Thus, orbits in this region move to bottom right and eventually cross the T_R nullcline to enter Region IV. In Region IV, $dT_h/dt < 0$ and $dT_R/dt < 0$. Thus, orbits in this region must monotonically approach the origin E_0. The phase portrait is illustrated in Fig. 6.

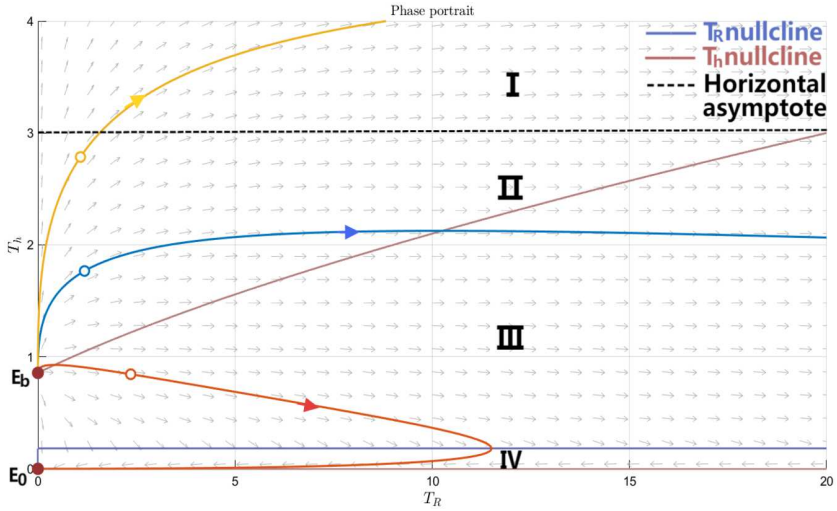

Figure 6: Phase portrait of model (4.1) under Subcase 3.2 of Case 3, where the parameters satisfy $\pi_h > \alpha_{10}+\alpha_\beta+\gamma+\mu_h$ and $\mu_R/\pi_R < \mu_h/\pi_h < 1$. The parameters used are $\pi_R=0.6, \mu_R=0.1, \pi_h=0.5, \mu_h=0.15, \alpha_{10}=\alpha_\beta=\gamma=0.1$.

Thus, in this subcase, the orbits above the boundary Γ must have $T_h(t)$ and $T_R(t)$ increase monotonically to ∞ with respect to time t. Orbits below Γ must have $T_h(t)$ monotonically decrease to 0 with respect to time t, while $T_R(t)$ also approaches 0, but undergoes an increase before doing so.

4.3.3 Subcase 3.3: $\mu_h/\pi_h < \mu_R/\pi_R < (\alpha_{10}+\alpha_\beta+\gamma+\mu_h)/\pi_h$

In this subcase, the T_R nullcline is between the boundary equilibrium E_b and the horizontal asymptote $T_h = T_h^\infty$ of the T_h nullcline. Thus, there exists a positive equilibrium $E^* = (T_h^*, T_R^*)$, and E_b is a saddle.

Proposition 4.2. *In this subcase, the stable manifold $w_+^s(E_b)$ is below the T_R nullcline* (4.4).

Proof. If $w_+^s(E_b)$ is above the T_R nullcline (4.4), then $dT_R/dt > 0$ on $w_+^s(E_b)$. Thus, $w_+^s(E_b)$ cannot approach the boundary equilibrium E_b, resulting in a contradiction. □

The horizontal asymptote $T_h = T_h^\infty$ of the T_h nullcline and $w_+^s(E_b)$ divide the first quadrant into three regions. Region I is above both the asymptote and $w_+^s(E_b)$. Region II is between them. Region III is below both. Like Region I in Subcase 3.2, orbits in Region I increase monotonically to ∞ with respect to time t. Also like Region III, orbits in Region III decrease monotonically to the origin E_0. Orbits in Region II are bounded below by $w_+^s(E_b)$ because the stable manifold is invariant. They may eventually enter Region I or approach the positive equilibrium E^*, depending on the locally stability of E^*. The phase portrait is illustrated in Fig. 7.

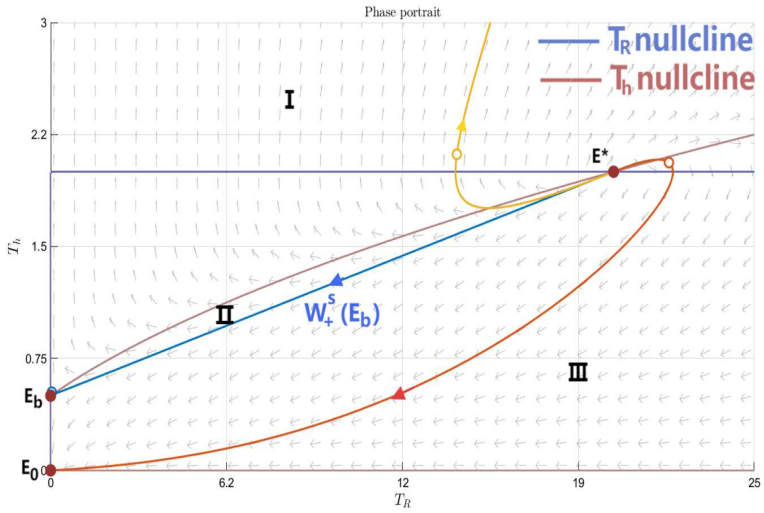

Figure 7: Phase portrait of model (4.1) under Subcase 3.3 of Case 3, where the parameters satisfy $\pi_h > \alpha_{10}+\alpha_\beta+\gamma+\mu_h$ and $\mu_h/\pi_h < \mu_R/\pi_R < (\alpha_{10}+\alpha_\beta+\gamma+\mu_h)/\pi_h$. The parameters used are $\pi_R=0.2, \mu_R=0.1$, $\pi_h=0.5, \mu_h=0.1, \alpha_{10}=\alpha_\beta=\gamma=0.1$.

4.3.4 Subcase 3.4: $(\alpha_{10}+\alpha_\beta+\gamma+\mu_h)/\pi_h < \mu_R/\pi_R$

In this subcase, because $\mu_h/\pi_h < (\alpha_{10}+\alpha_\beta+\gamma+\mu_h)/\pi_h < \mu_R/\pi_R$, the boundary equilibrium E_b is a saddle. In addition, the T_R nullcline (4.4) is above the horizontal asymptote $T_h = T_h^\infty$ of the T_h nullcline (4.3). Thus, there is no positive equilibrium.

Note that, in this subcase, Proposition 4.1 still holds. Thus, the two nullclines ((4.3)-(4.4)) and the stable manifold $w^s_+(E_b)$ divide the first quadrant into four regions. Region I is above the nullclines (and thus above $w^s_+(E_b)$). Region II is between the two nullclines. Region III is between the T_h nullcline and $w^s_+(E_b)$. Region IV is below $w^s_+(E_b)$.

In Region I, $dT_h/dt > 0$ and $dT_R/dt > 0$, and thus, as in Region I of Subcase 3.1, the orbits in this region increase monotonically to ∞ with respect to time t. In Region II, $dT_h/dt > 0$ and $dT_R/dt < 0$. Thus, orbits in this region move towards top-left, and eventually enter Region I. In both Regions III and IV, $dT_h/dt < 0$ and $dT_R/dt < 0$. Thus, the orbits move towards bottom left. However, in Region III, they are bounded below by $w^s_+(E_b)$, and thus must eventually enter Region II. In Region IV, the orbits approach the origin E_0 monotonically. The phase portrait is illustrated in Fig. 8.

Thus, in this subcase, orbits above $w^s_+(E_b)$ eventually have $T_h(t)$ and $T_R(t)$ both increasing monotonically to ∞. Orbits below $w^s_+(E_b)$ cause both $T_h(t)$ and $T_R(t)$ to decrease monotonically to 0.

The following theorem summarizes the dynamics of model (4.1) in this case. Specifically, if the initially activated CD4+ T cell population is below a threshold defined by $w^s_+(E_b)$, then there is no significant CD4+ T cell response. On the other hand, once the threshold is surpassed, the immune response cannot be eliminated after infection.

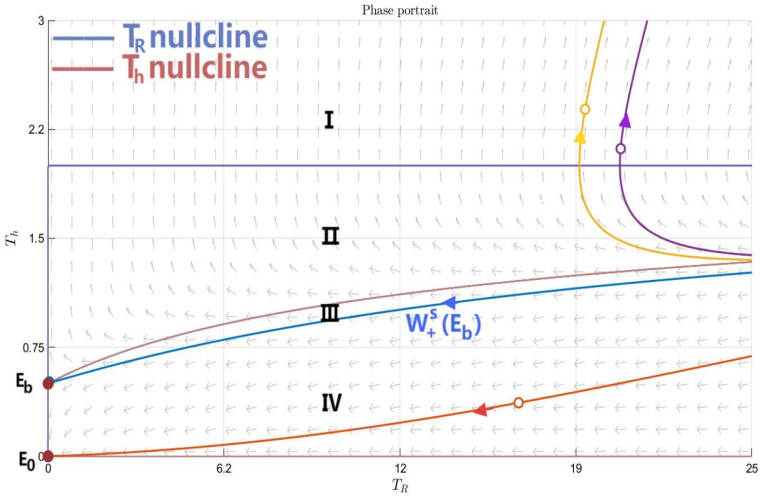

Figure 8: Phase portrait of model (4.1) under Subcase 3.4 of Case 3, where the parameters satisfy $\pi_h > \alpha_{10}+\alpha_\beta+\gamma+\mu_h$ and $(\alpha_{10}+\alpha_\beta+\gamma+\mu_h)/\pi_h < \mu_R/\pi_R$. The parameters used are $\pi_R=0.2, \mu_R=0.1, \pi_h=0.5$, $\mu_h=0.1, \alpha_{10}=\alpha_\beta=0.00625, \gamma=0.1$.

Theorem 4.4. *In Case* 3*, orbits of the model* (4.1) *below* $w^s_+(E_b)$ *have* $T_h(t)$ *and* $T_R(t)$ *decreasing monotonically to* 0*; orbits above* $w^s_+(E_b)$ *remain above it, and may have* $T_h(t)$ *and* $T_R(t)$ *increasing monotonically to* ∞*.*

5 Conclusion

Without regulation, the positive feedback of the autocrine action of activated CD4+ T cells and IL-2 leads to uncontrollable growth if the proliferation rate exceeds the rate of cell death, and the initial population size is greater than a threshold. This is in agreement with that in [26], and clearly demonstrates the importance of regulating the proliferation process. Multiple biological mechanisms for such regulation exist. We performed a comprehensive study to identify the key regulation mechanism on the regulation of CD4+ T cell proliferation in the autopilot model. Using mathematical models, we separately considered both the self-regulation of IL-2 and the effects of Tregs. For both, we have considered the reduction in IL-2 production and the increase in cell apoptosis, albeit resulting from different biological mechanisms.

We found that IL-2 self-regulation of reduced IL-2 production at a high IL-2 concentration cannot regulate the uncontrollable autocrine proliferation of CD4+ T cells. On the other hand, increased CD4+ T cell mortality at a high IL-2 concentration causes the proliferation of CD4+ T cells to reach homeostasis. However, this mechanism does not facilitate the clearance of the CD4+ immune response after infection. These results suggest that these mechanisms are complementary and cannot be the key mechanism to guarantee clearance of the immune response post infection.

We showed that Treg inhibition of IL-2 production and elevation of CD4+ T cell apoptosis together provide the necessary mechanisms to regulate CD4+ T cell proliferation. These mechanisms may result in a regulated CD4+ T cell immune response. However, this is only achievable if the total effect of inhibiting activated CD4+ cells from producing IL-2 and CD4+ T cell death dominates the proliferation rate of CD4+ T cells. In this case, the proliferation is an excitable process, i.e. if the initial activated CD4+ T cell population exceeds a threshold, proliferation starts automatically, peaks, and eventually clears. However, if the proliferation rate is not dominated, some initial conditions lead to uncontrollable expansion where the CD4+ T cell population approaches infinity.

Zhang *et al.* [26] also demonstrated the excitable nature of CD4+ T cell proliferation. However, due to the unrealistic assumption of bilinear (i.e. unsaturated) regulation, their model results in a perpetually controllable CD4+ T cell proliferation process as long as Treg cells proliferate faster than their deaths. Our result is more realistic because the regulation process depends on regulatory cytokines such as IL-10 and TGF-β binding to CD4+ T cell receptors. The binding process depletes these receptors, causing saturation at high cytokine concentrations.

The combined effects of Treg cell regulation and IL-2 self-regulation have not been accounted for in this study. Due to the intricate interplay between these two immune response mechanisms, involving multi-level feedback regulation, the mathematical analysis of the resulting mathematical model is challenging. To understand the combined effects of these mechanisms on the immune response, further investigation is needed, and it presents an interesting avenue for future research. This study is primarily theoretical in nature, aiming to establish the qualitative dynamics of the model under mathematically consistent parameter sets rather than fitting to experimental data. Calibration with empirical data represents a crucial next step and will be addressed in future work, with a focus on the application of the model to specific biological systems.

Acknowledgements

This work was supported by the Natural Sciences and Engineering Research Council Canada (Grant No. RGPIN-2025-06907) (J. Ma), by the National Natural Science Foundation of China (Grant No. 12271088) (M. Li), by the Natural Science Foundation of Shanghai (Grant Nos. 21ZR1401000, 23ZR1401700) (M. Li), and by the Donghua University (X. Li).

References

[1] B. B. Au-Yeung, J. Zikherman, J. L. Mueller, J. F. Ashouri, M. Matloubian, D. A. Cheng, Y. Chen, K. M. Shokat, and A. Weiss, *A sharp T-cell antigen receptor signaling threshold for T-cell proliferation*, Proc. Natl. Acad. Sci. USA, 111:E3679–E3688, 2014.

[2] R. N. Bamford, A. J. Grant, J. D. Burton, C. Peters, G. Kurys, C. K. Goldman, J. Brennan, E. Roessler, and T. Waldmann, *The interleukin (IL) 2 receptor beta chain is shared by IL-2 and*

a cytokine, provisionally designated IL-T, that stimulates T-cell proliferation and the induction of lymphokine-activated killer cells, Proc. Natl. Acad. Sci. USA, 91:4940–4944, 1994.
[3] M. J. Bevan and P. J. Fink, *The CD8 response on autopilot*, Nat. Immunol., 2:381–382, 2001.
[4] J. A. Bluestone and Q. Tang, *T_{reg} cells – the next frontier of cell therapy*, Science, 362:154–155, 2018.
[5] W. Chen, *TGF-β regulation of T cells*, Annu. Rev. Immunol., 41:483–512, 2023.
[6] L. Cuesta-Herrera, L. Pastenes, A. D. Arencibia, F. Córdova-Lepe, and C. Montoya, *Dynamics of activation and regulation of the immune response to attack by viral pathogens using mathematical modeling*, Mathematics, 12:2681, 2024.
[7] K. García-Martínez and K. León, *Modeling the role of IL-2 in the interplay between CD4+ helper and regulatory T cells: Assessing general dynamical properties*, J. Theor. Biol., 262:720–732, 2010.
[8] D. Gong and T. Malek, *Cytokine-dependent Blimp-1 expression in activated T cells inhibits IL-2 production*, J. Immunol., 178:242–252, 2007.
[9] Z. Grossman and W. E. Paul, *Adaptive cellular interactions in the immune system: The tunable activation threshold and the significance of subthreshold responses*, Proc. Natl. Acad. Sci. USA, 89:10365–10369, 1992.
[10] H. Gudmundsdottir, A. D. Wells, and L. A. Turka, *Dynamics and requirements of T cell clonal expansion in vivo at the single-cell level: Effector function is linked to proliferative capacity*, J. Immunol., 162:5212–5223, 1999.
[11] P. Hsu, B. Santner-Nanan, M. Hu, K. Skarratt, C. H. Lee, M. Stormon, M. Wong, S. J. Fuller, and R. Nanan, *Il-10 potentiates differentiation of human induced regulatory T cells via STAT3 and Foxo1*, J. Immunol., 195:3665–3674, 2015.
[12] M. Huse, *The T-cell-receptor signaling network*, J. Cell Sci., 122:1269–1273, 2009.
[13] S. M. Kaech and R. Ahmed, *Memory CD8+ T cell differentiation: Initial antigen encounter triggers a developmental program in naive cells*, Nat. Immunol., 2:415–422, 2001.
[14] V. Kalia, S. Sarkar, S. Subramaniam, W. N. Haining, K. A. Smith, and R. Ahmed, *Prolonged interleukin-2rα expression on virus-specific CD8+ T cells favors terminal-effector differentiation in vivo*, Immunity, 32:91–103, 2010.
[15] B. J. Kaskow and C. Baecher-Allan, *Effector T cells in multiple sclerosis*, Cold Spring Harb. Perspect. Med., 8(4):a029025, 2018.
[16] S. Khailaie, F. Bahrami, M. Janahmadi, P. Milanez-Almeida, J. Huehn, and M. Meyer-Hermann, *A mathematical model of immune activation with a unified self-nonself concept*, Front Immunol., 4:474, 2013.
[17] P. Khalili and R. Vatankhah, *Studying the importance of regulatory T cells in chemoimmunotherapy mathematical modeling and proposing new approaches for developing a mathematical dynamic of cancer*, J. Theor. Biol., 563:111437, 2023.
[18] T. R. Malek, *The biology of interleukin-2*, Annu. Rev. Immunol., 26:453–479, 2008.
[19] K. Murphy and C. Weaver, *Janeway's Immunobiology*, Garland Science, 2016.
[20] B. H. Nelson, *Il-2, regulatory T cells, and tolerance*, J. Immunol., 172:3983–3988, 2004.
[21] L. V. Parijs and A. K. Abbas, *Homeostasis and self-tolerance in the immune system: Turning lymphocytes off*, Science, 280:243–248, 1998.
[22] S. Roy, M. Ren, S. Christensen, P. Li, R. Spolski, J. Phelan, L. Staudt, and W. J. Leonard, *Blimp-1 is a negative regulator of IL-2 signaling in T cells*, J. Immunol., 210(Supplement_1):243.01, 2023.
[23] A. H. Sharpe, *Mechanisms of costimulation*, Immunol. Rev., 229:5–11, 2009.
[24] M. J. van Stipdonk, E. E. Lemmens, and S. P. Schoenberger, *Naive CTLs require a single brief period of antigenic stimulation for clonal expansion and differentiation*, Nat. Immunol., 2:423–429, 2001.

[25] Y. Wakabayashi et al., *Histone 3 lysine 9 (H3K9) methyltransferase recruitment to the interleukin-2 (IL-2) promoter is a mechanism of suppression of IL-2 transcription by the transforming growth factor-β-Smad pathway*, J. Biol. Chem., 286(41):35456—35465, 2011.
[26] M. Zhang, J. Ma, R. Edwards, and M. Li, *The dynamics of CD4+ T cell proliferation and regulation*, J. Biol. Dyn., 19:2458867, 2025.
[27] Y. Zhang, P. B. Alexander, and X.-F. Wang, *TGF-β family signaling in the control of cell proliferation and survival*, Cold Spring Harb. Perspect. Biol., 9(4):a022145, 2017.
[28] J. Zhu, H. Yamane, and W. E. Paul, *Differentiation of effector CD4 T cell populations*, Annu. Rev. Immunol., 28:445–489, 2010.